WFG5 3M 8d

Fig. 1: Example of found solutions on WFG5 with $M = 3$, $d = 8$. Comparison between SAF_{EI} and -SAF_{μ} above, and SAF_{μ} and SMS-EGO below. Solutions found after 150 evaluations and with identical starting conditions.
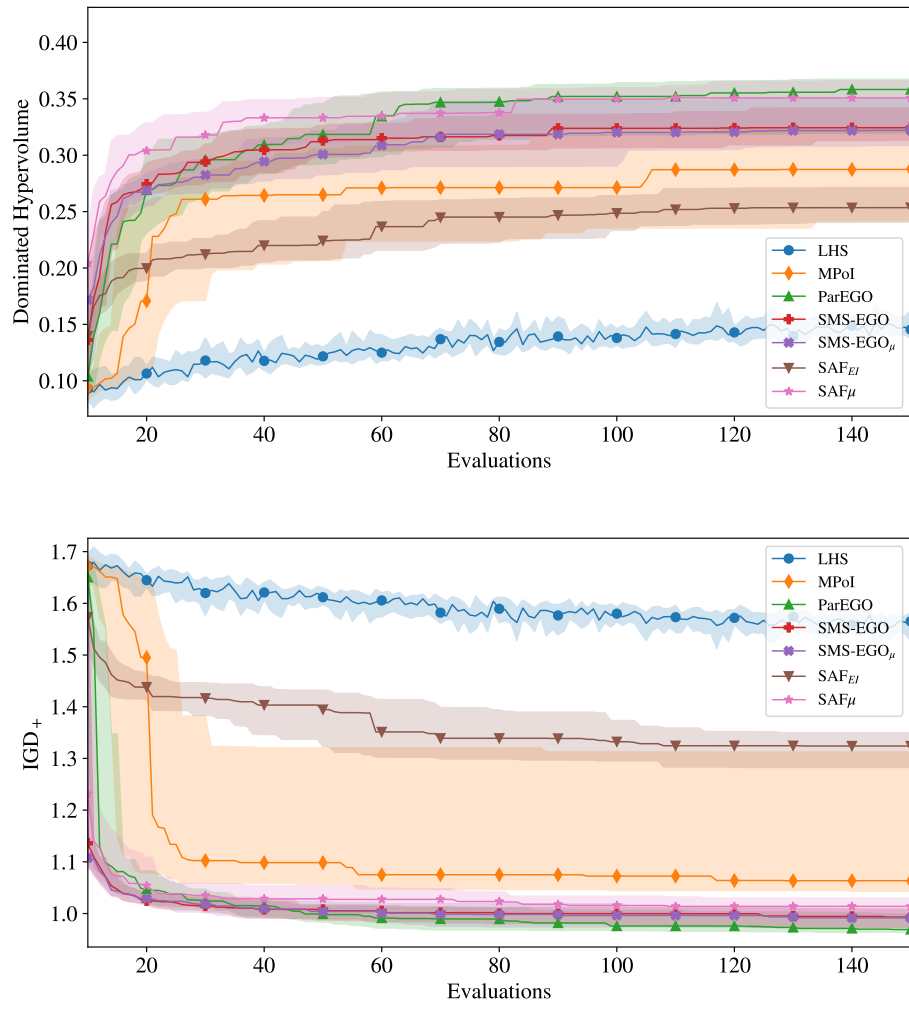
Fig. 2: Convergence plots showing median Dominated Hypervolume and IGD+ over 31 repeats. IQR shown in shaded region. Dominated hypervolume calculated as a fraction of the maximum possible.
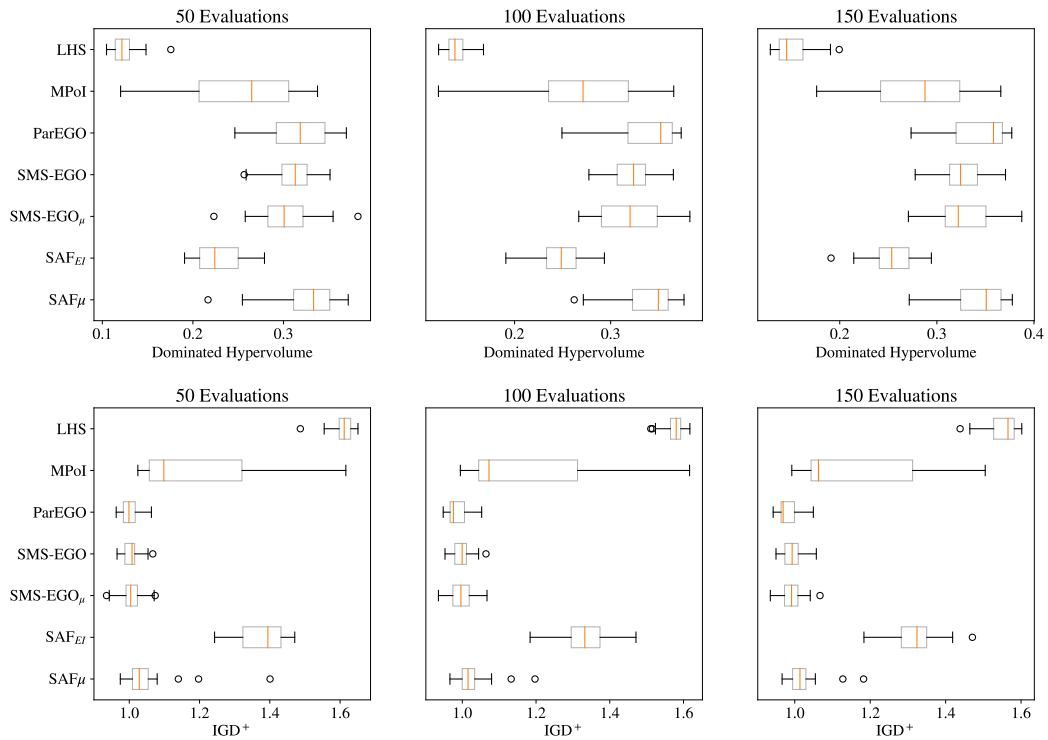

Fig. 3: Box plots showing Dominated Hypervolume and IGD+ over 31 repeats at three stages of the optimisation process.
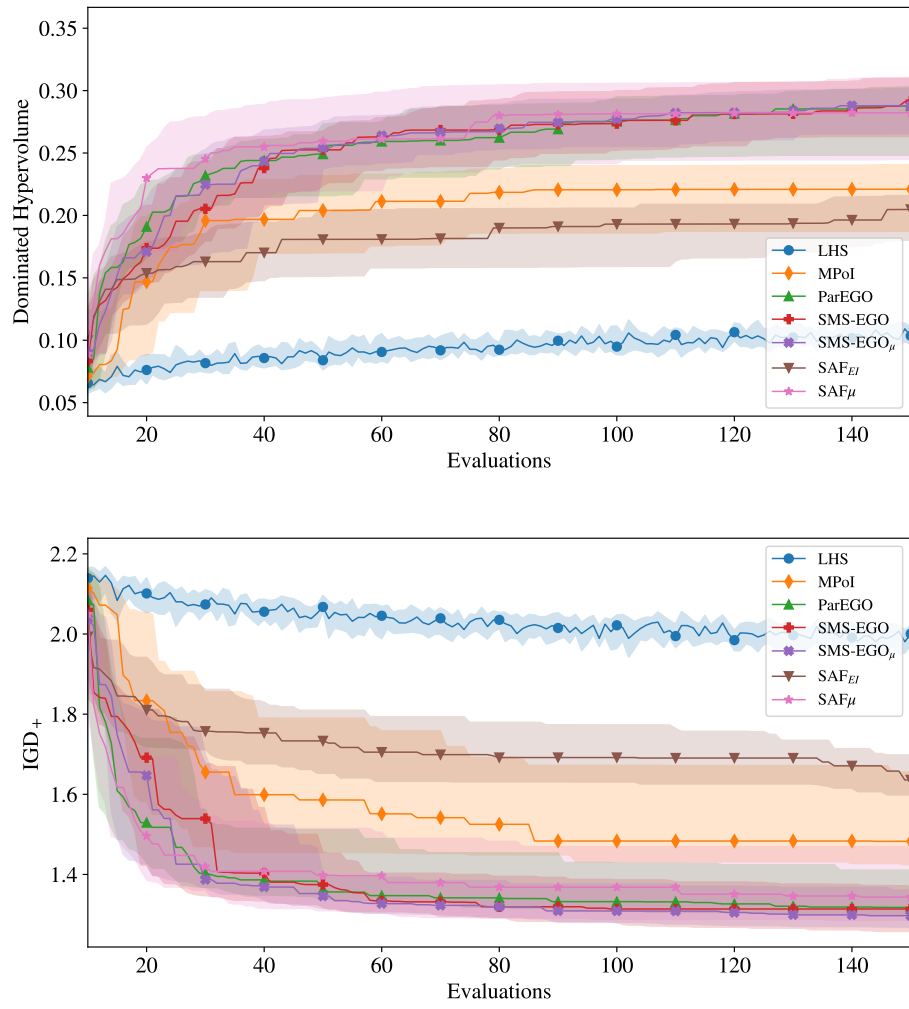
Fig. 4: Convergence plots showing median Dominated Hypervolume and IGD+ over 31 repeats. IQR shown in shaded region. Dominated hypervolume calculated as a fraction of the maximum possible.
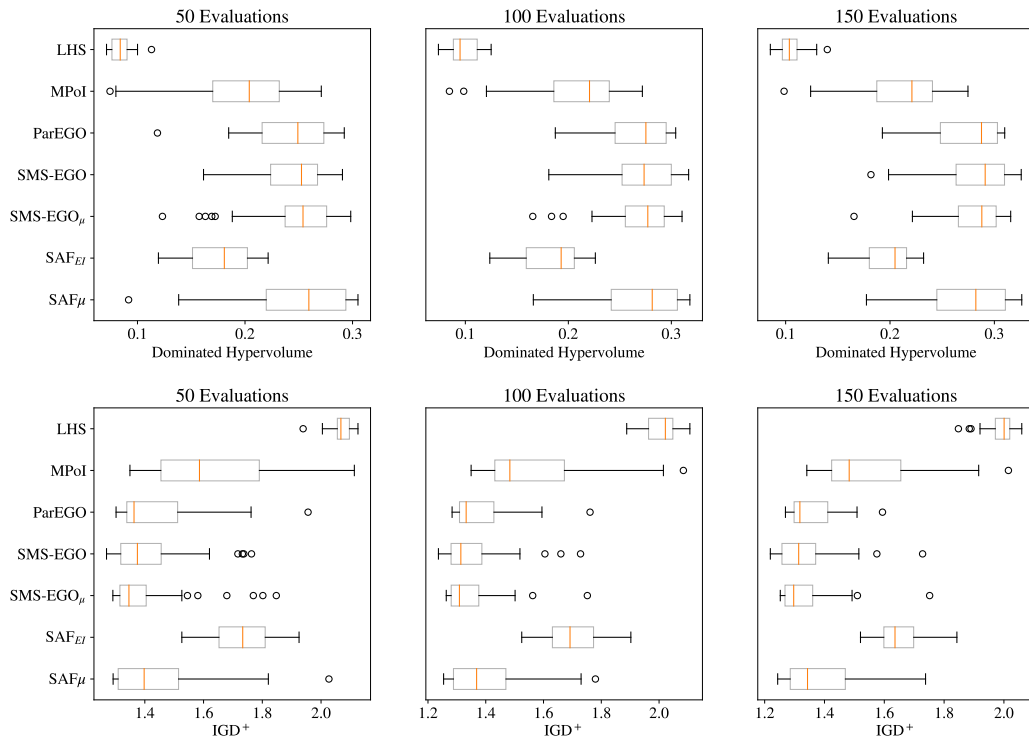

Fig. 5: Box plots showing Dominated Hypervolume and IGD+ over 31 repeats at three stages of the optimisation process.
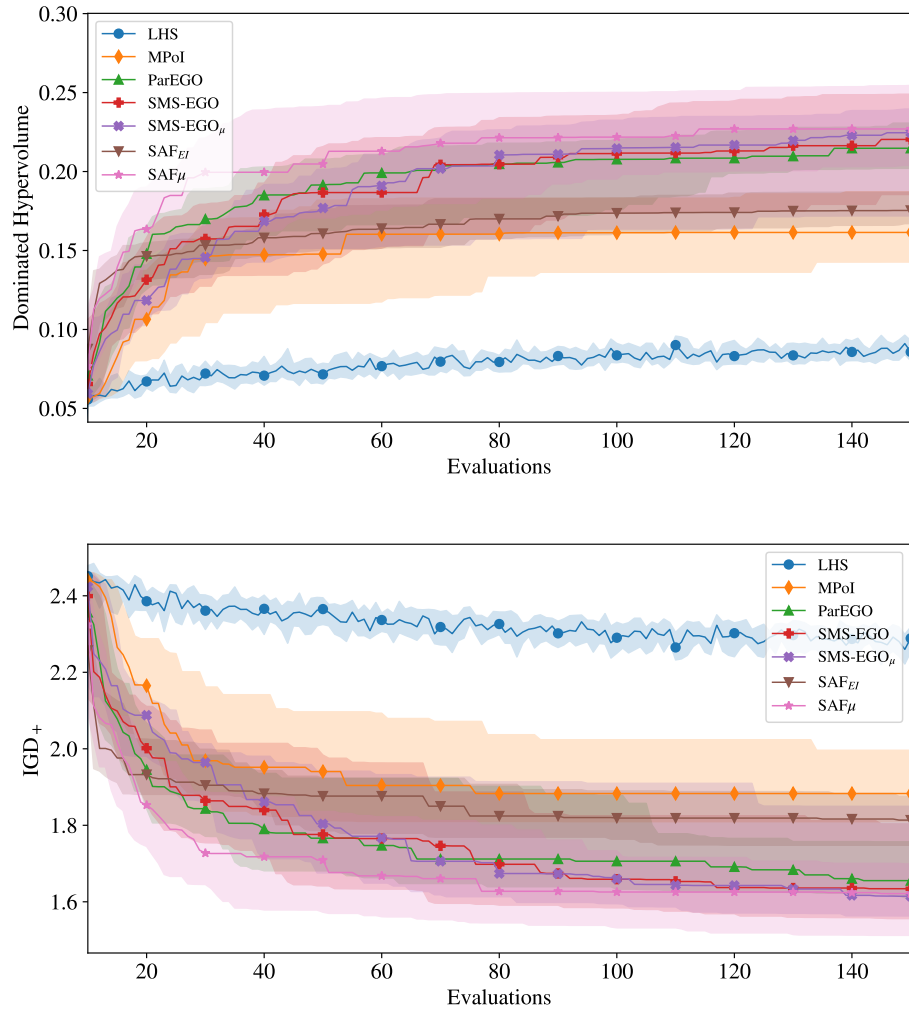
Fig. 6: Convergence plots showing median Dominated Hypervolume and IGD+ over 31 repeats. IQR shown in shaded region. Dominated hypervolume calculated as a fraction of the maximum possible.
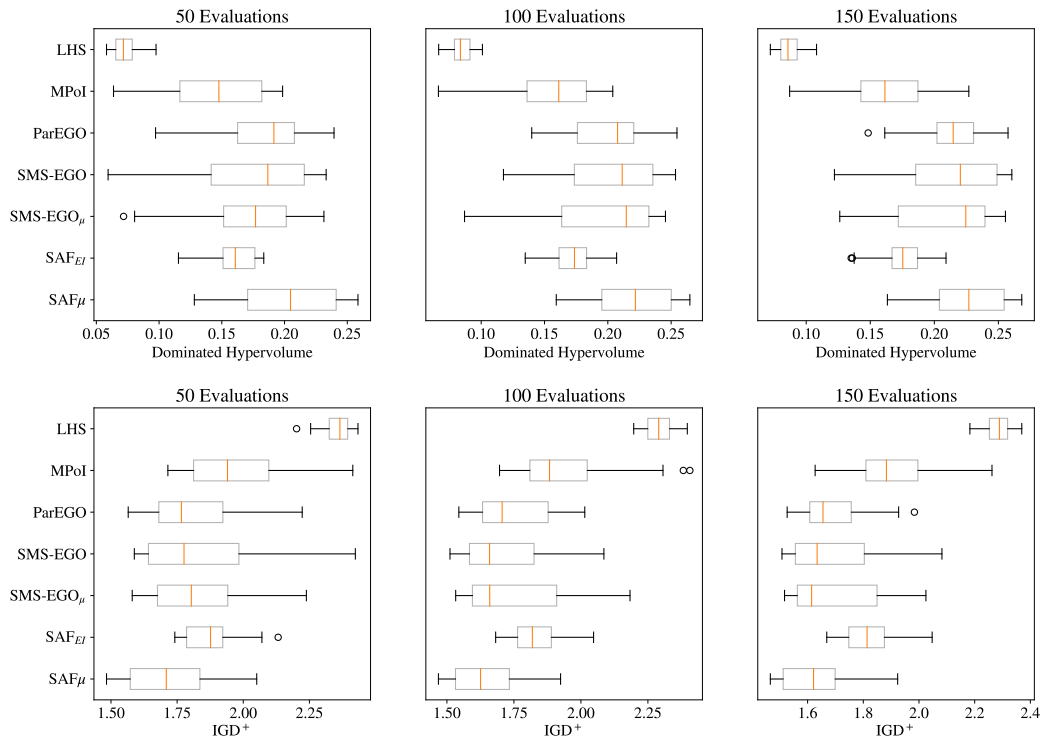

Fig. 7: Box plots showing Dominated Hypervolume and IGD+ over 31 repeats at three stages of the optimisation process.
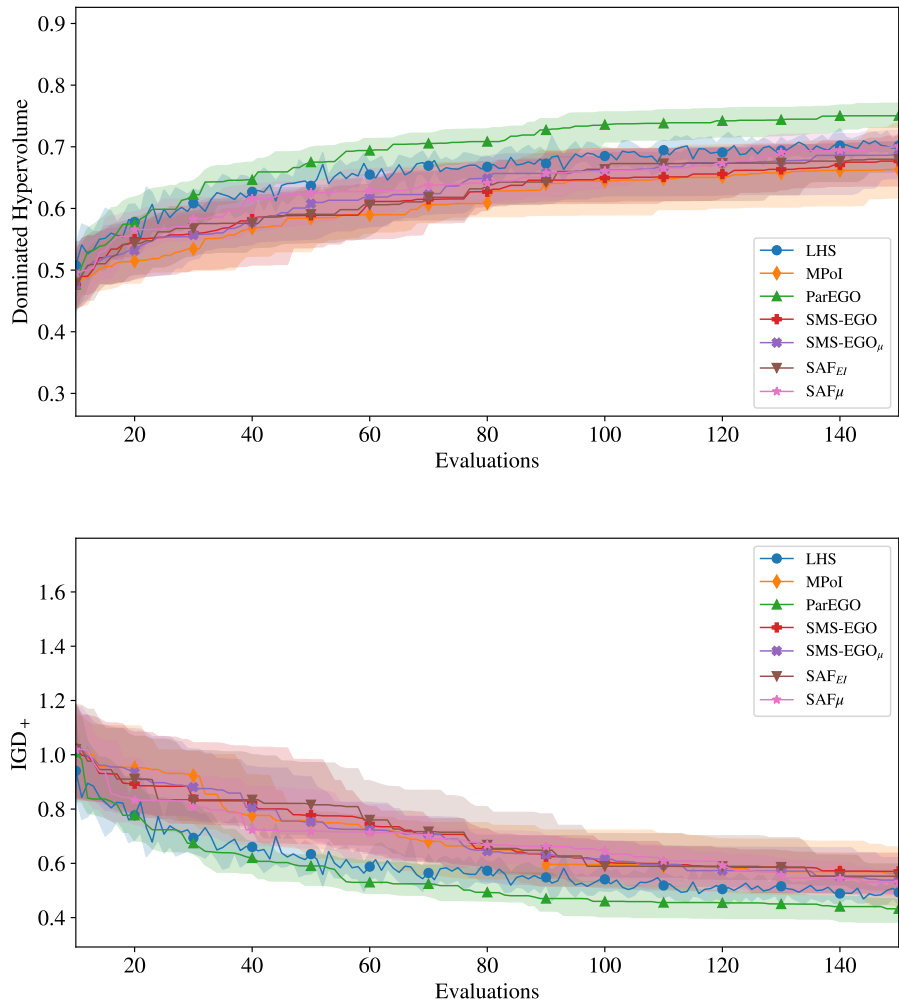
Fig. 8: Convergence plots showing median Dominated Hypervolume and IGD+ over 31 repeats. IQR shown in shaded region. Dominated hypervolume calculated as a fraction of the maximum possible.
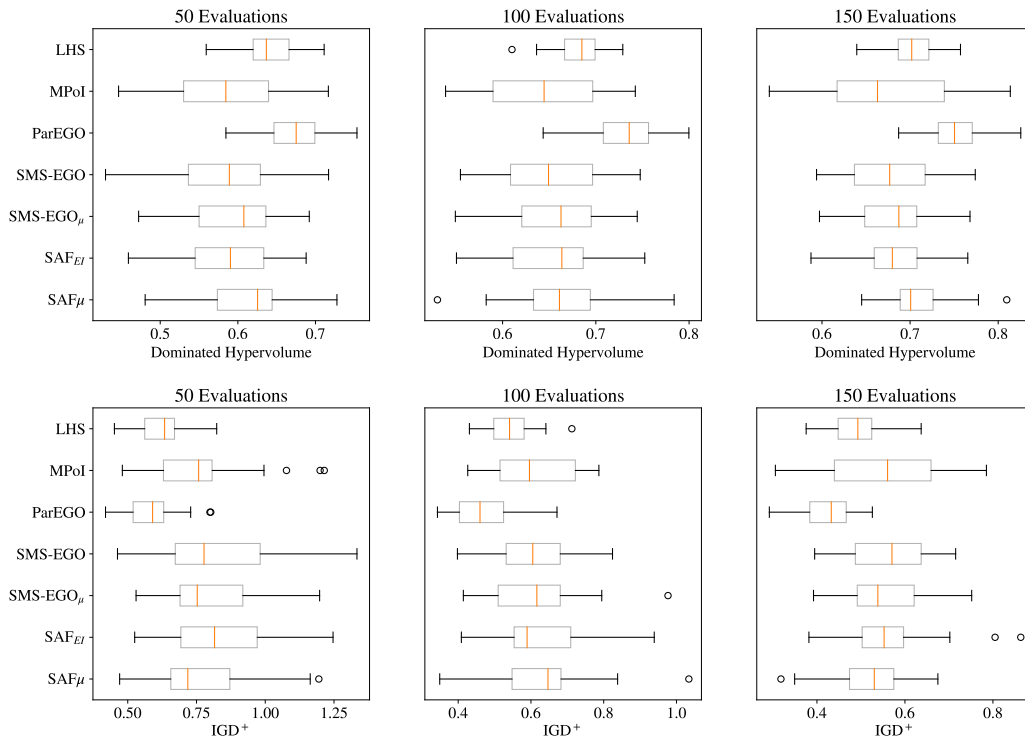

Fig. 9: Box plots showing Dominated Hypervolume and IGD+ over 31 repeats at three stages of the optimisation process.
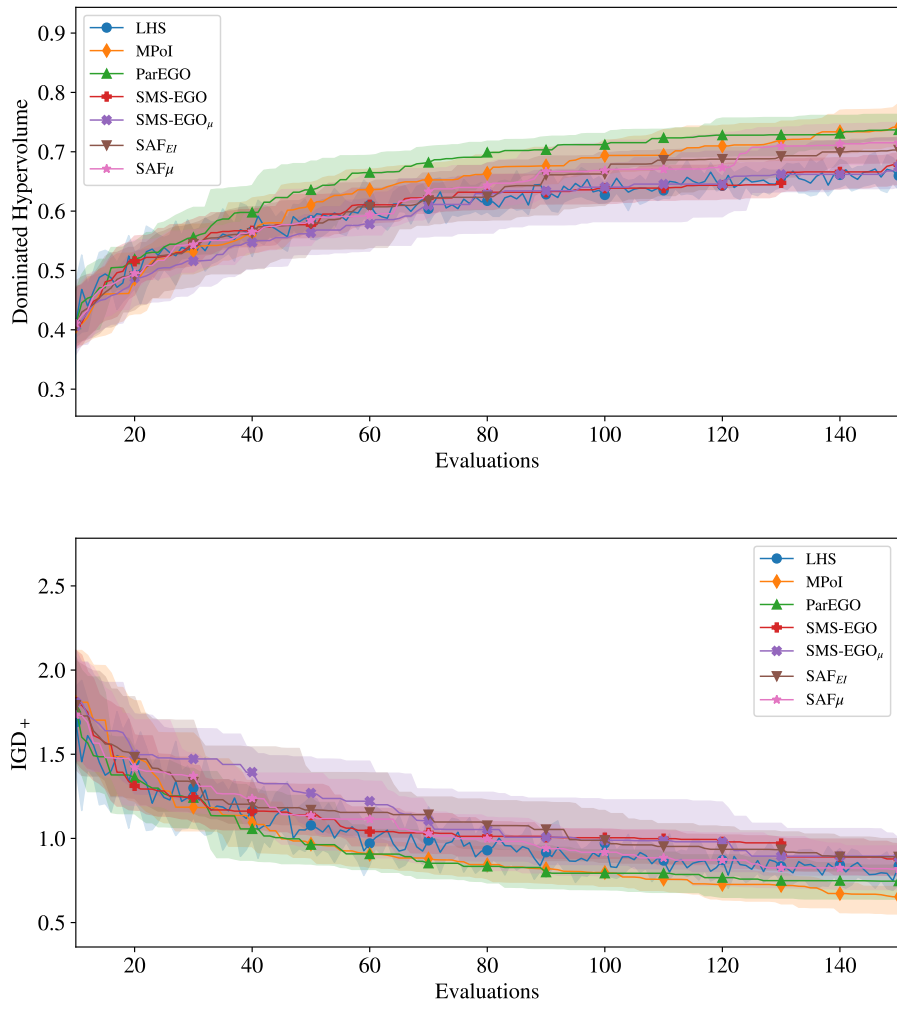
Fig. 10: Convergence plots showing median Dominated Hypervolume and IGD+ over 31 repeats. IQR shown in shaded region. Dominated hypervolume calculated as a fraction of the maximum possible.
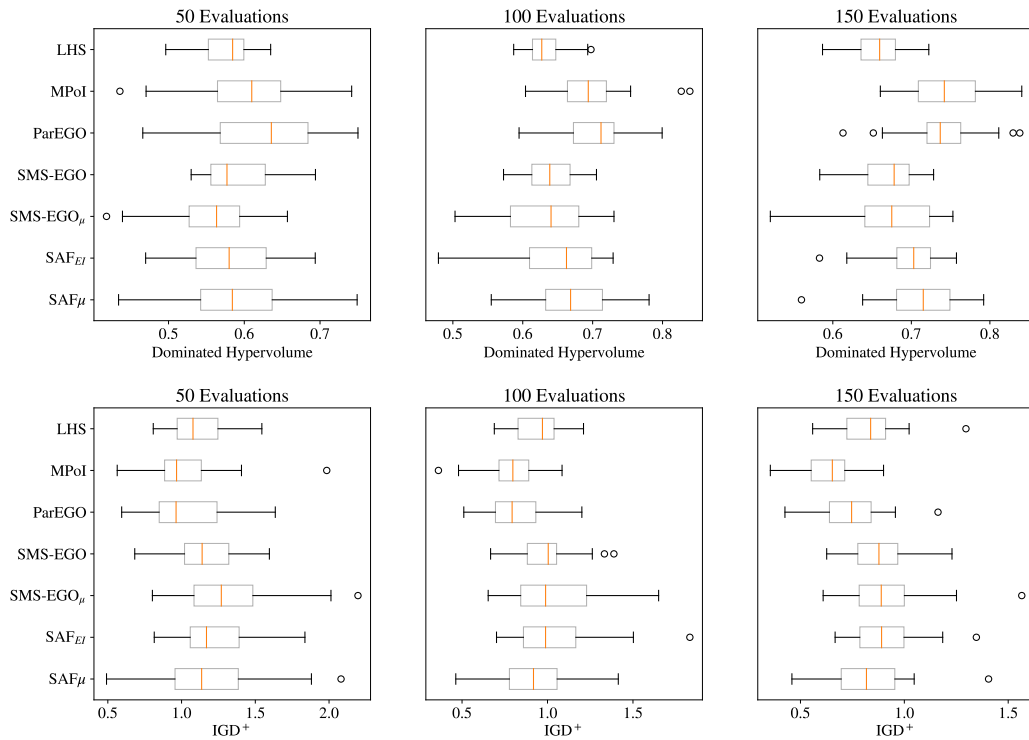

Fig. 11: Box plots showing Dominated Hypervolume and IGD+ over 31 repeats at three stages of the optimisation process.
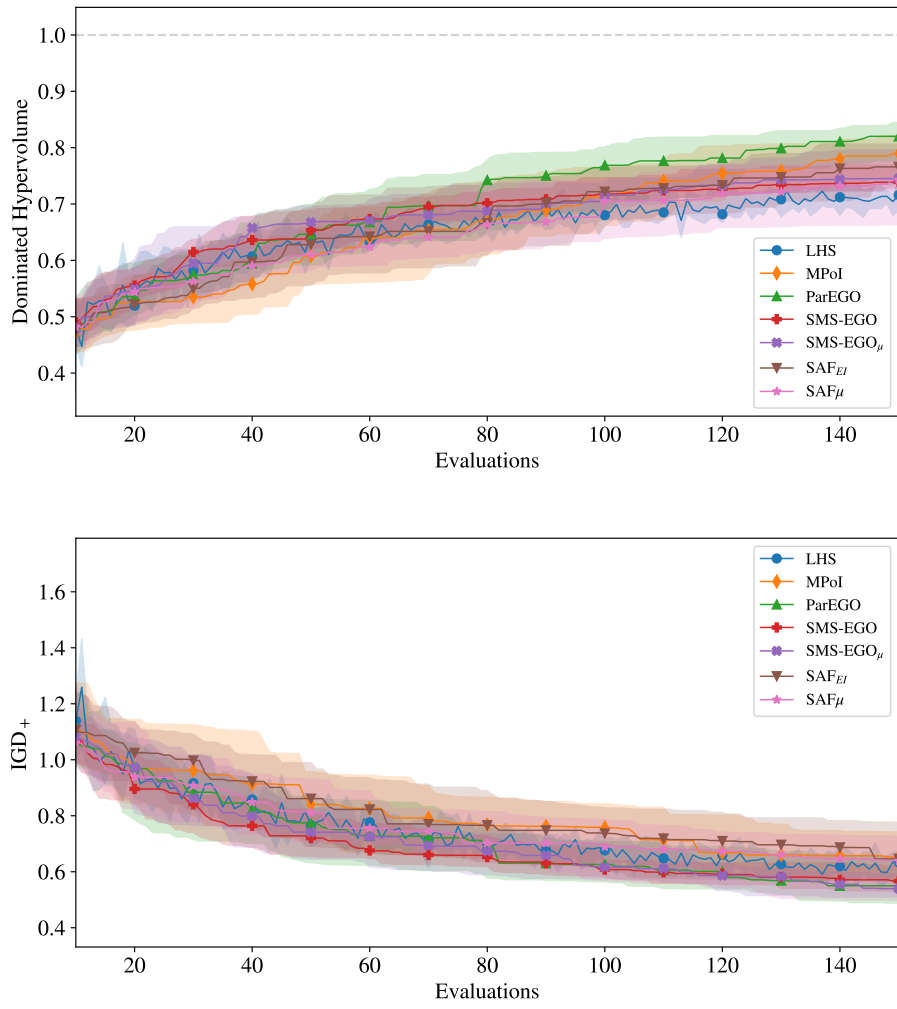
Fig. 12: Convergence plots showing median Dominated Hypervolume and IGD+ over 31 repeats. IQR shown in shaded region. Dominated hypervolume calculated as a fraction of the maximum possible.
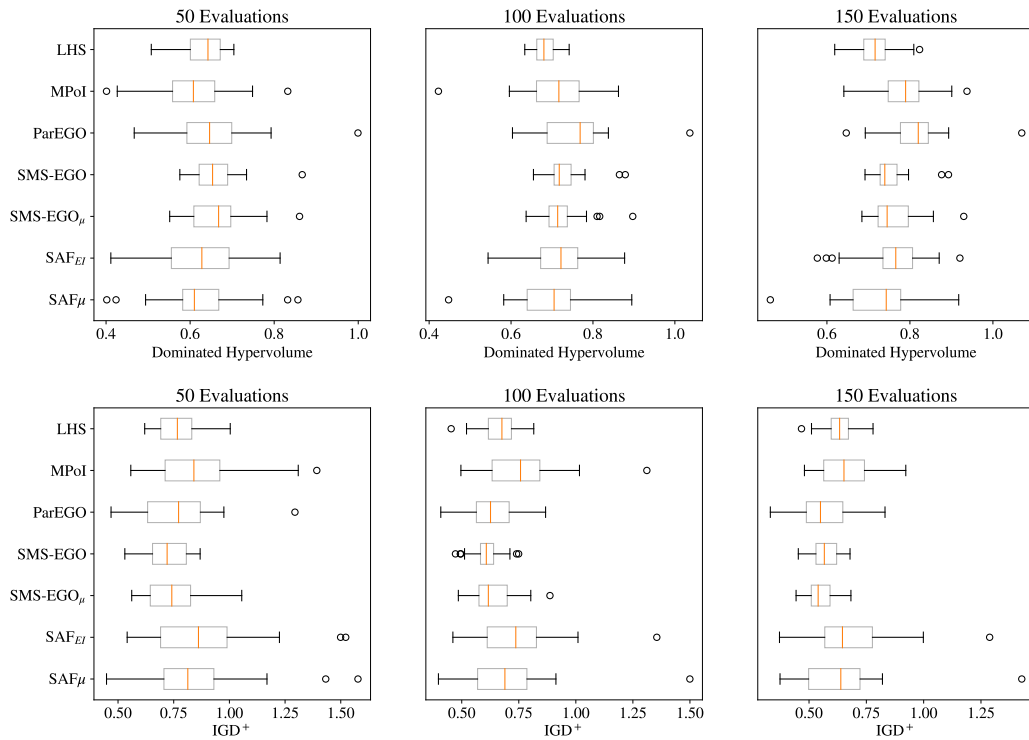

Fig. 13: Box plots showing Dominated Hypervolume and IGD+ over 31 repeats at three stages of the optimisation process.
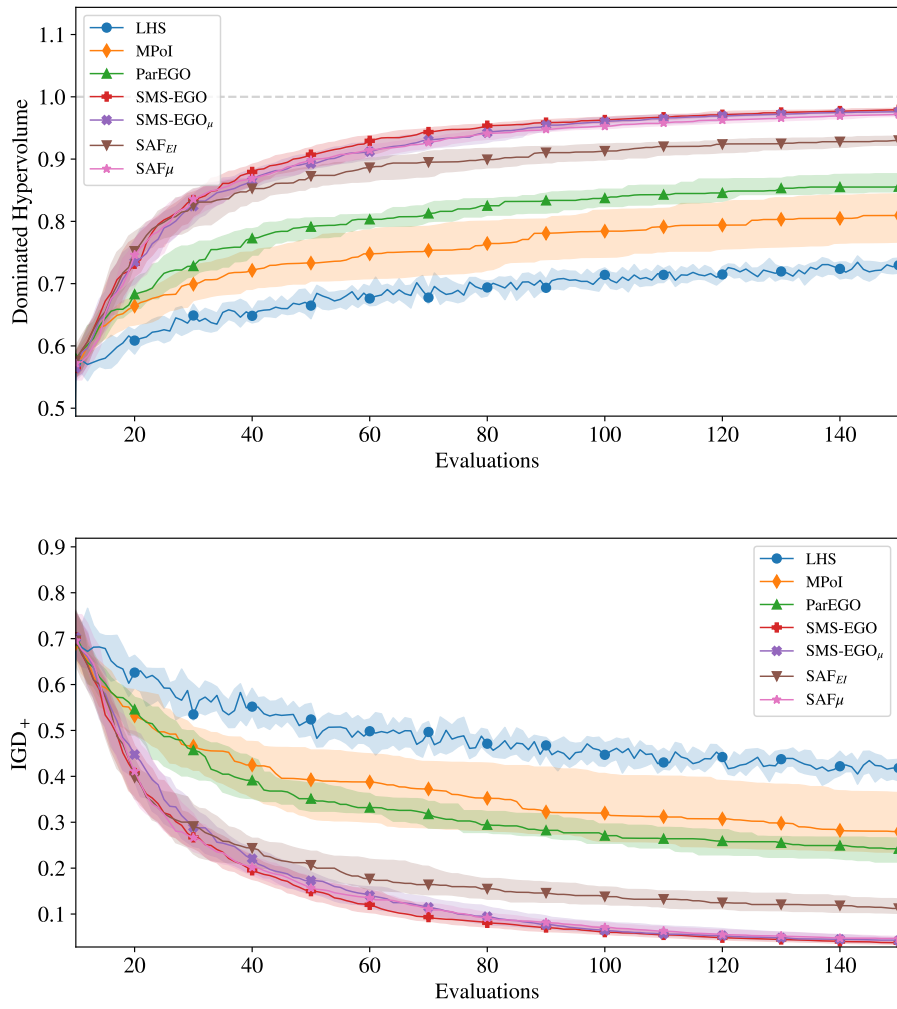
Fig. 14: Convergence plots showing median Dominated Hypervolume and IGD+ over 31 repeats. IQR shown in shaded region. Dominated hypervolume calculated as a fraction of the maximum possible.
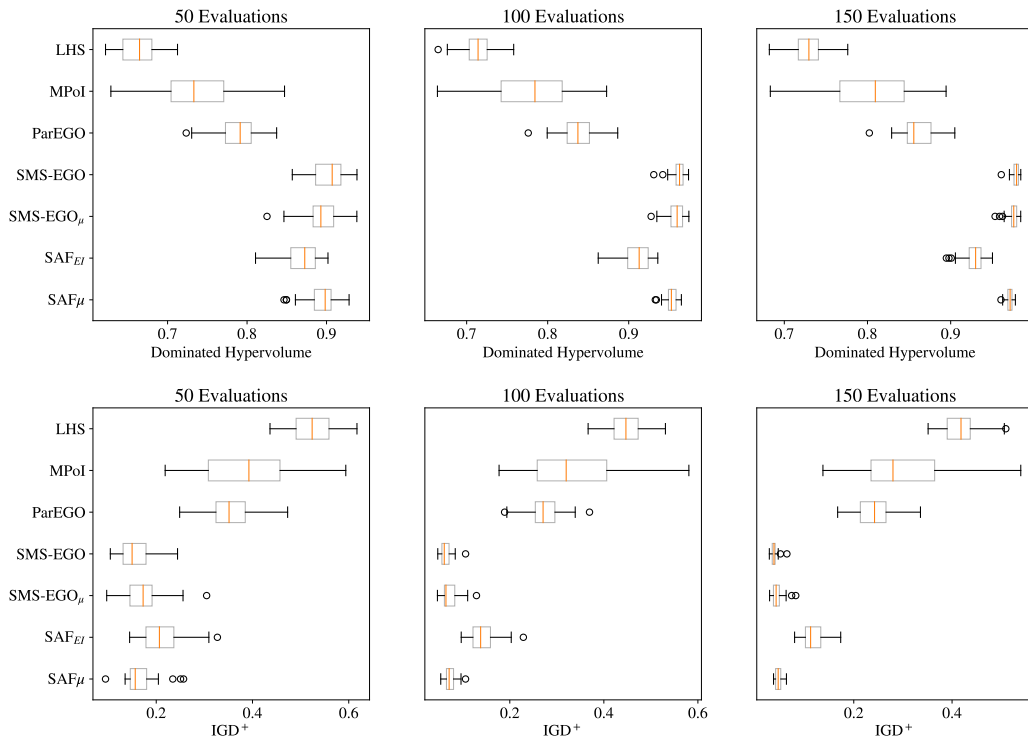

Fig. 15: Box plots showing Dominated Hypervolume and IGD+ over 31 repeats at three stages of the optimisation process.
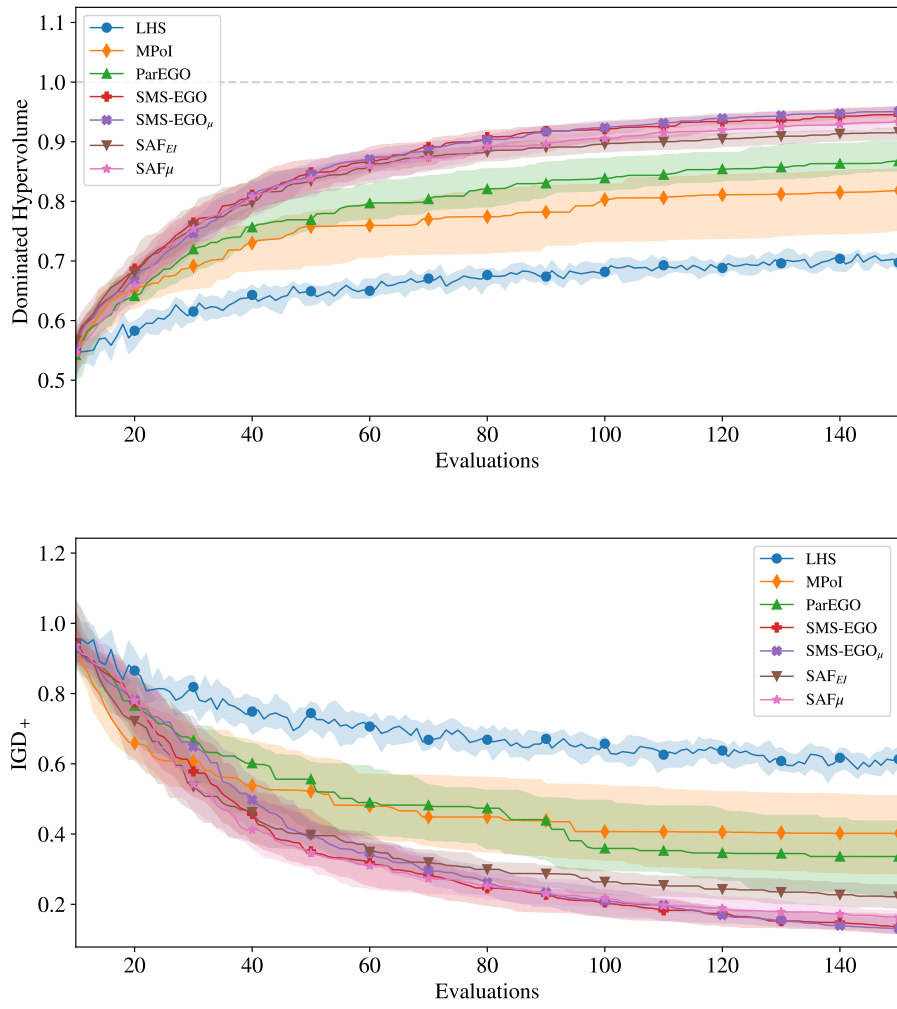
Fig. 16: Convergence plots showing median Dominated Hypervolume and IGD+ over 31 repeats. IQR shown in shaded region. Dominated hypervolume calculated as a fraction of the maximum possible.
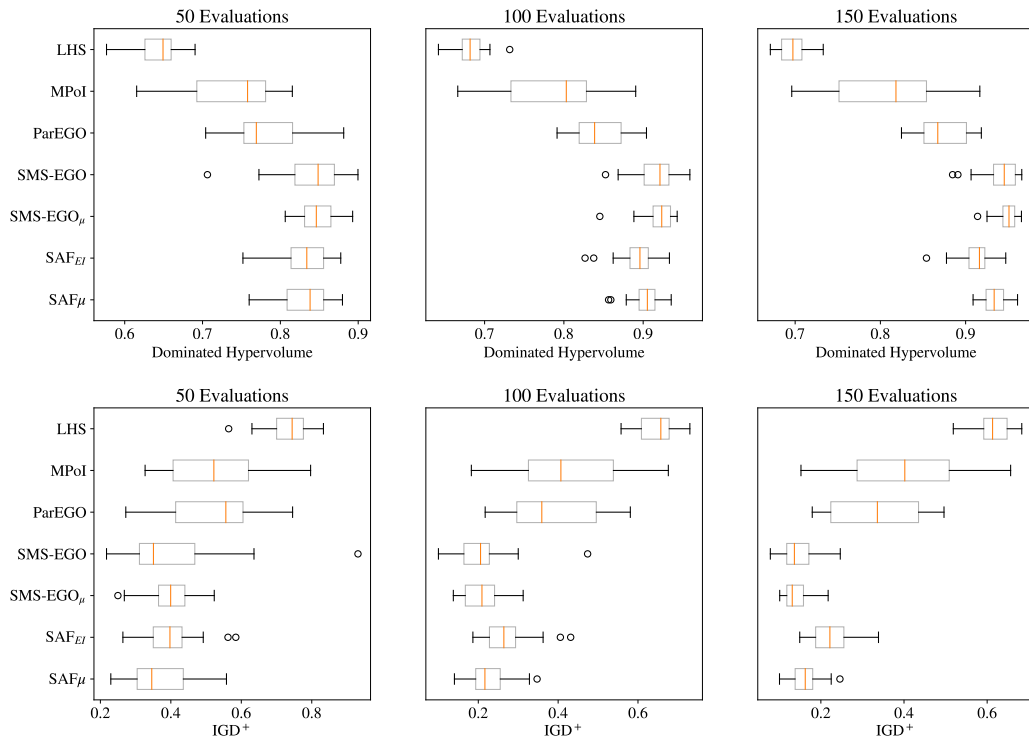

Fig. 17: Box plots showing Dominated Hypervolume and IGD+ over 31 repeats at three stages of the optimisation process.
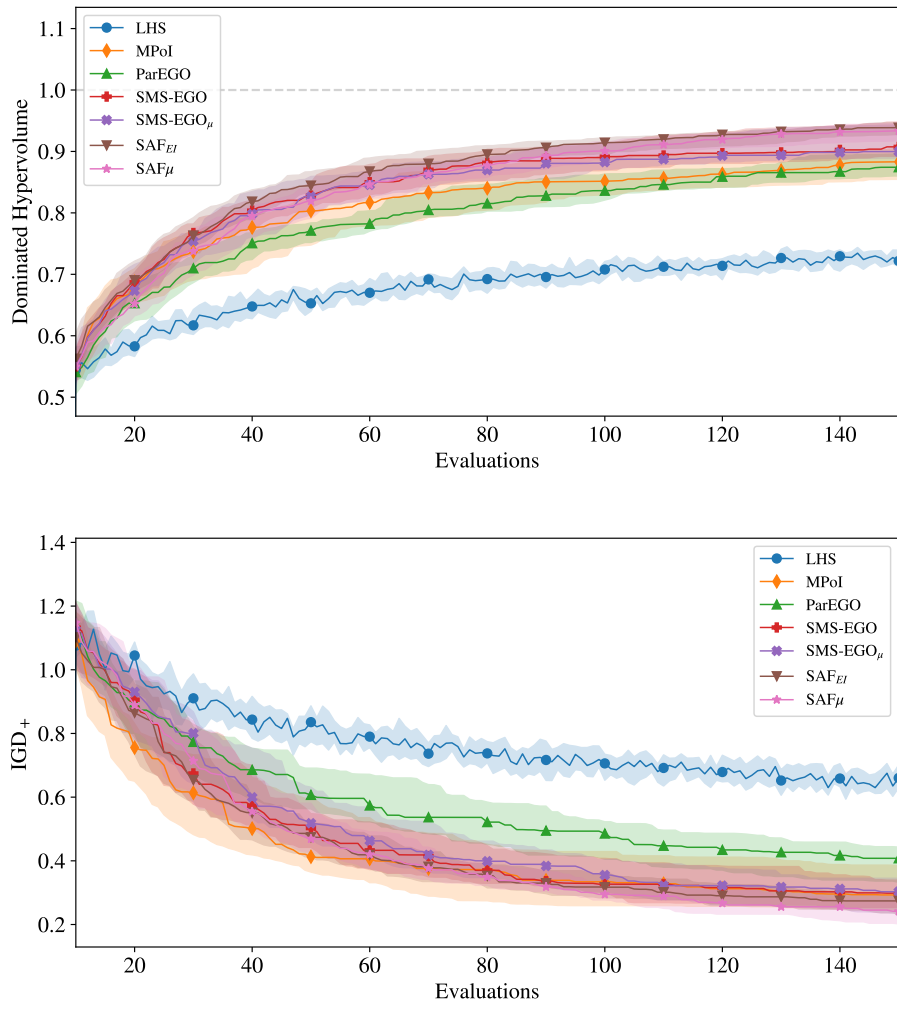
Fig. 18: Convergence plots showing median Dominated Hypervolume and IGD+ over 31 repeats. IQR shown in shaded region. Dominated hypervolume calculated as a fraction of the maximum possible.
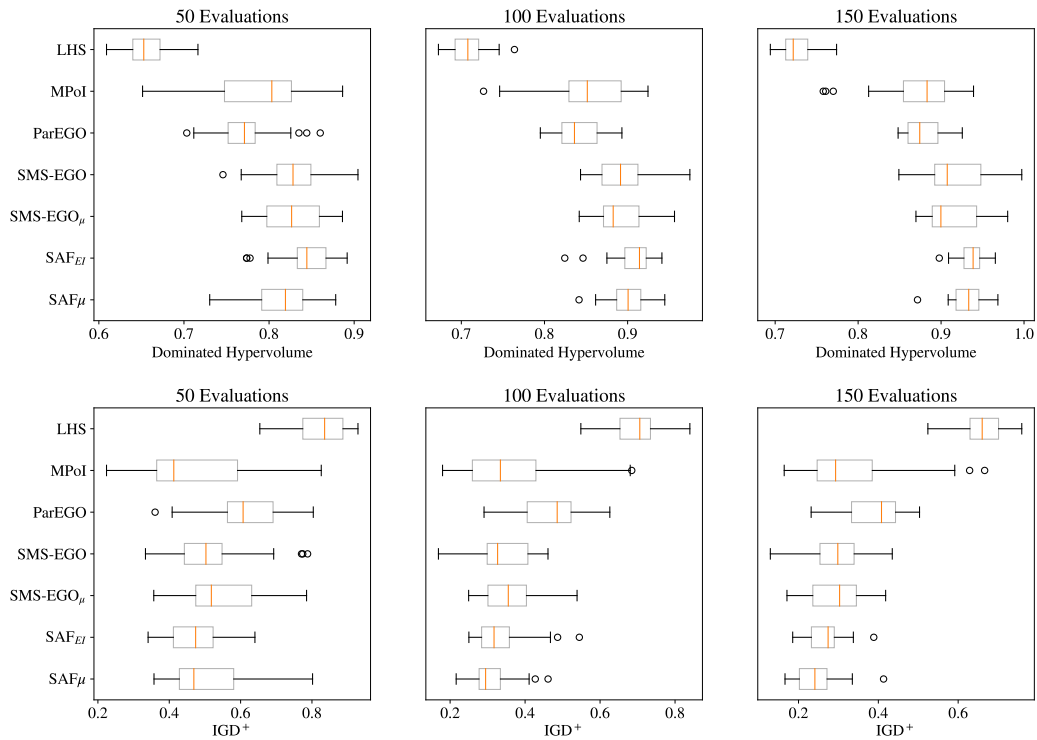

Fig. 19: Box plots showing Dominated Hypervolume and IGD+ over 31 repeats at three stages of the optimisation process.
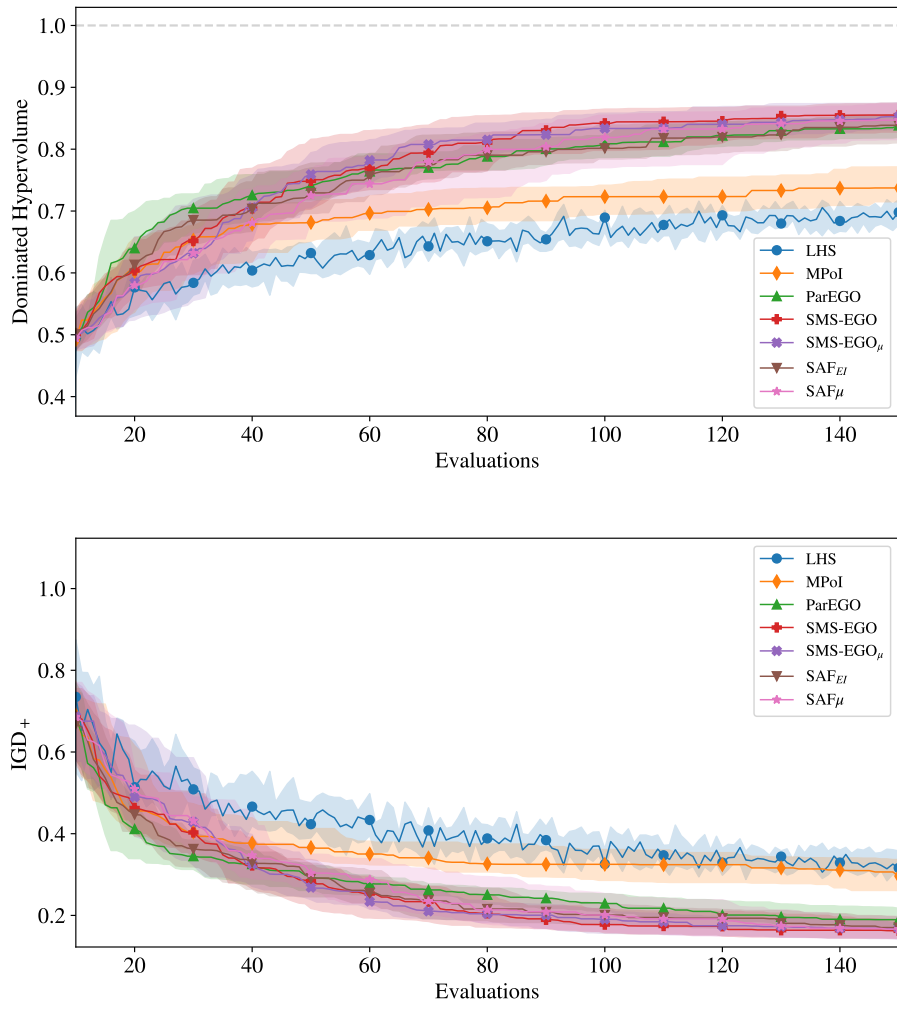
Fig. 20: Convergence plots showing median Dominated Hypervolume and IGD+ over 31 repeats. IQR shown in shaded region. Dominated hypervolume calculated as a fraction of the maximum possible.
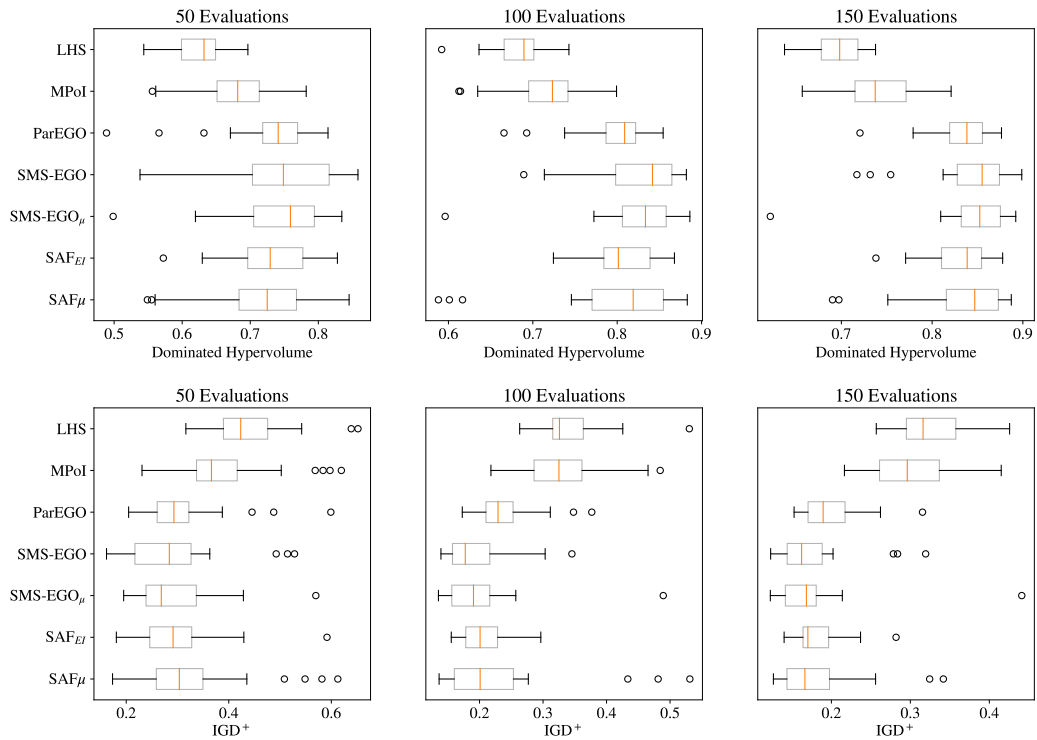

Fig. 21: Box plots showing Dominated Hypervolume and IGD+ over 31 repeats at three stages of the optimisation process.
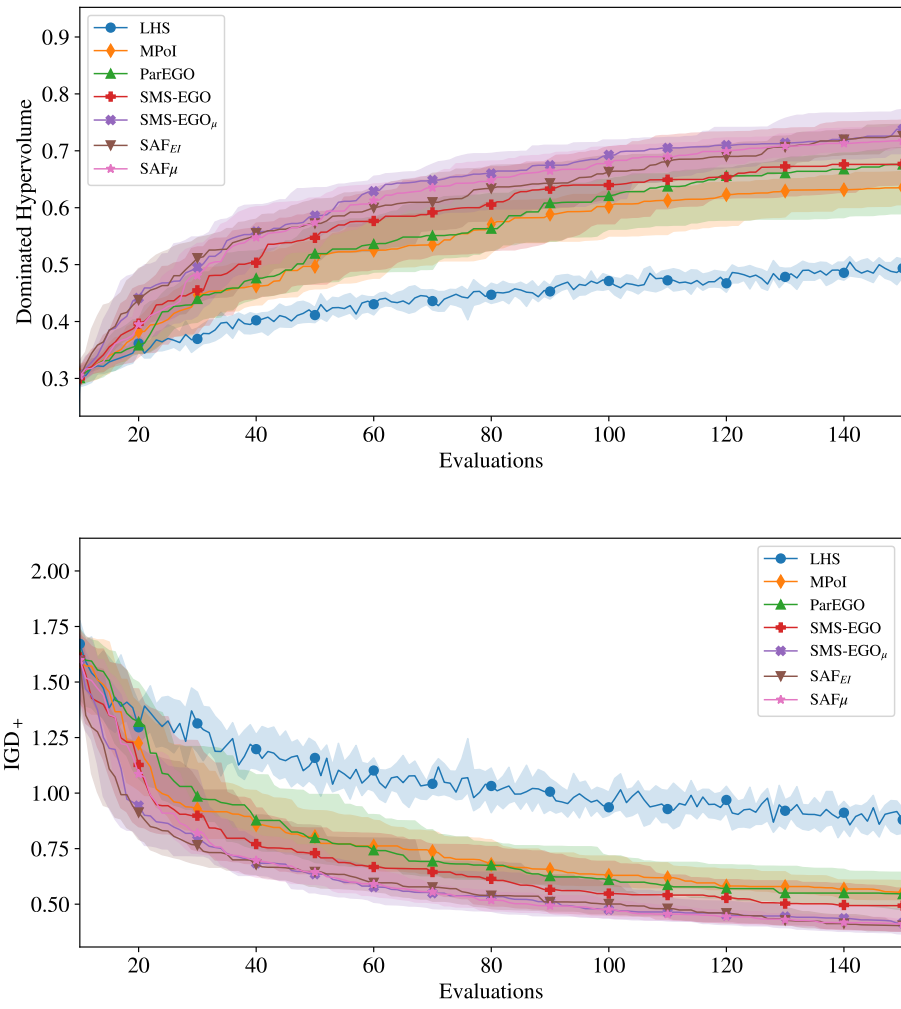
Fig. 22: Convergence plots showing median Dominated Hypervolume and IGD+ over 31 repeats. IQR shown in shaded region. Dominated hypervolume calculated as a fraction of the maximum possible.
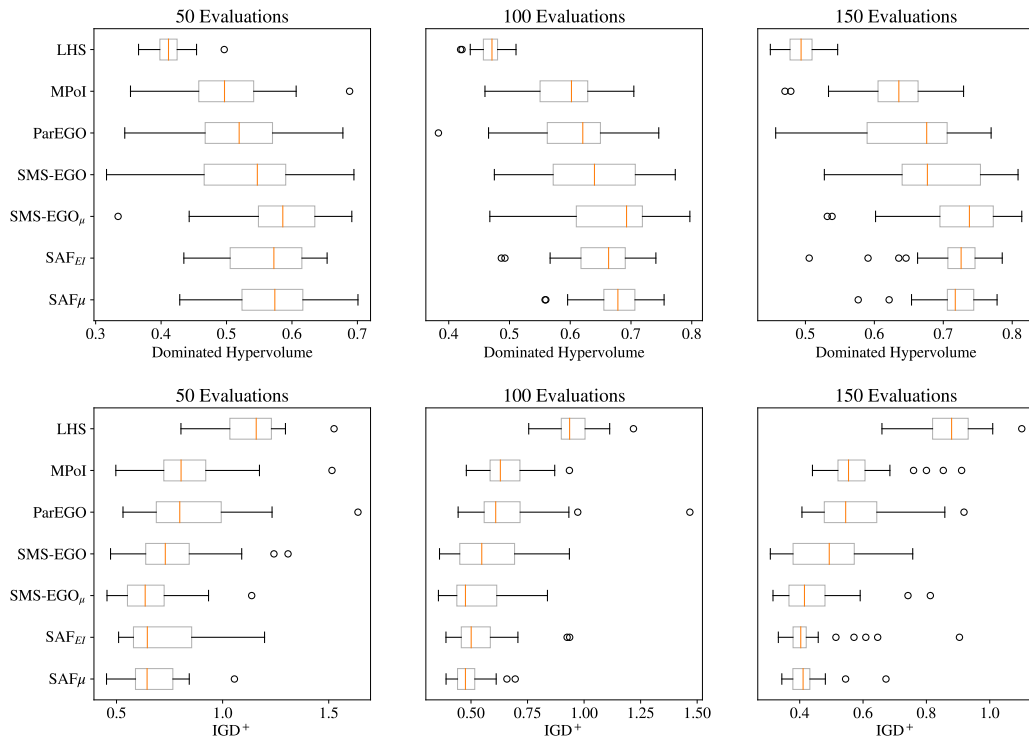

Fig. 23: Box plots showing Dominated Hypervolume and IGD+ over 31 repeats at three stages of the optimisation process.
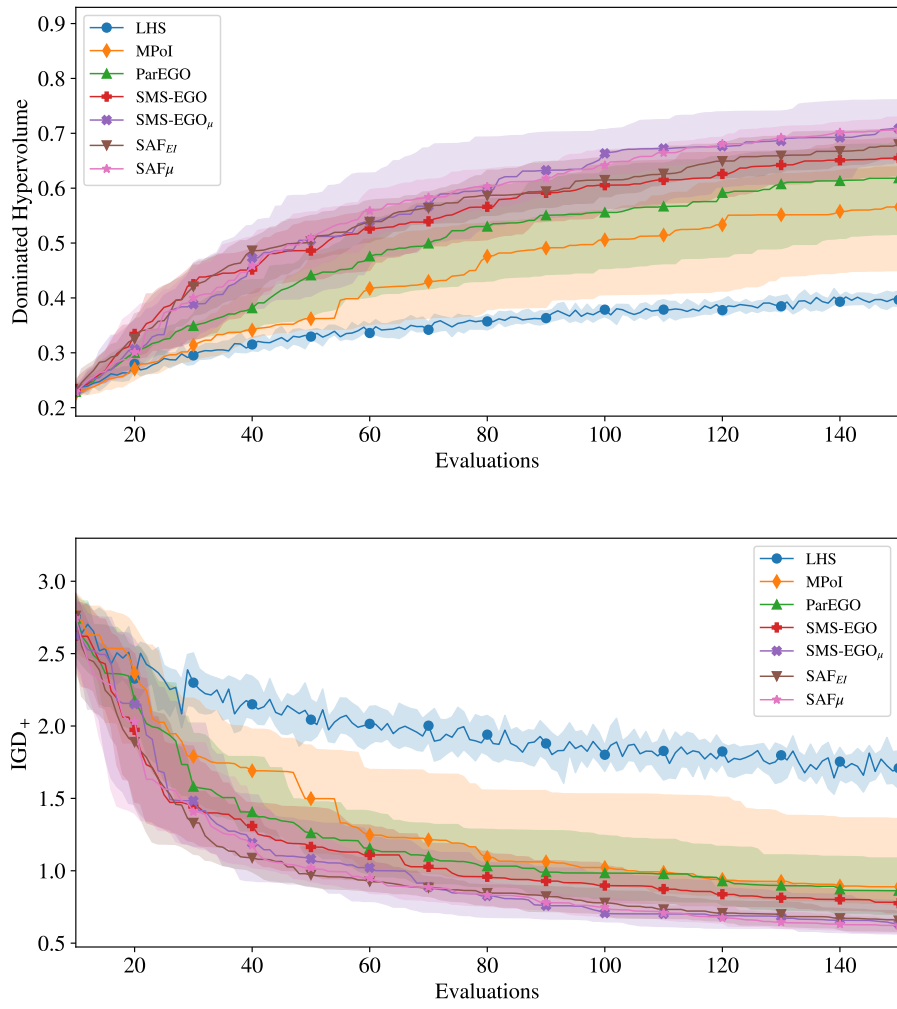
Fig. 24: Convergence plots showing median Dominated Hypervolume and IGD+ over 31 repeats. IQR shown in shaded region. Dominated hypervolume calculated as a fraction of the maximum possible.
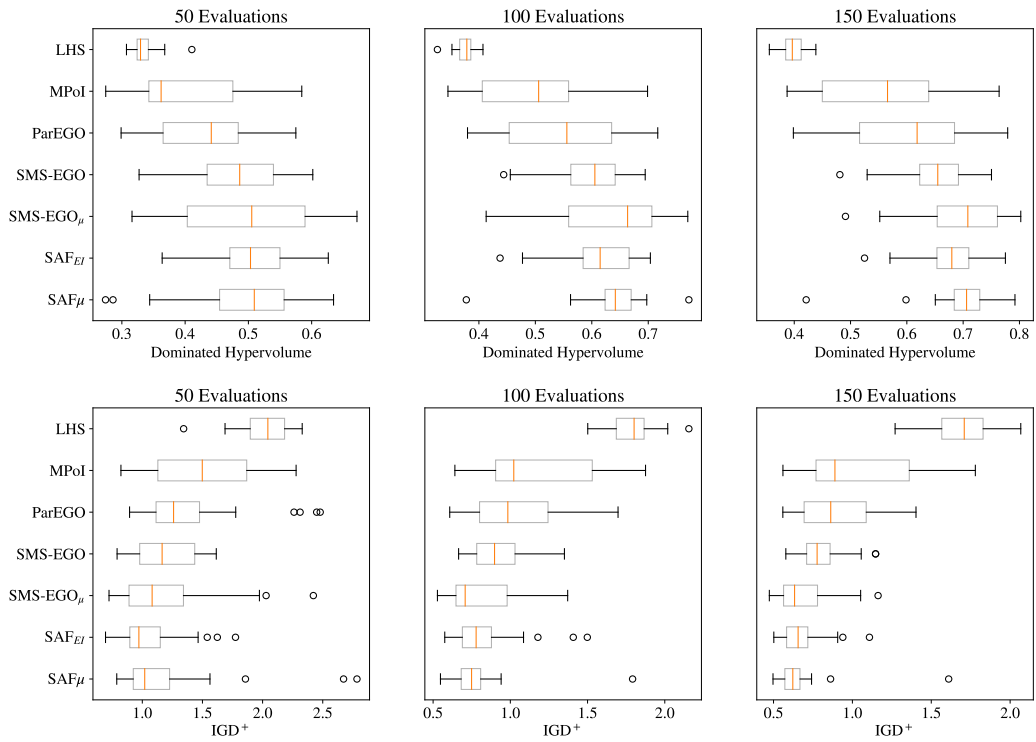

Fig. 25: Box plots showing Dominated Hypervolume and IGD+ over 31 repeats at three stages of the optimisation process.
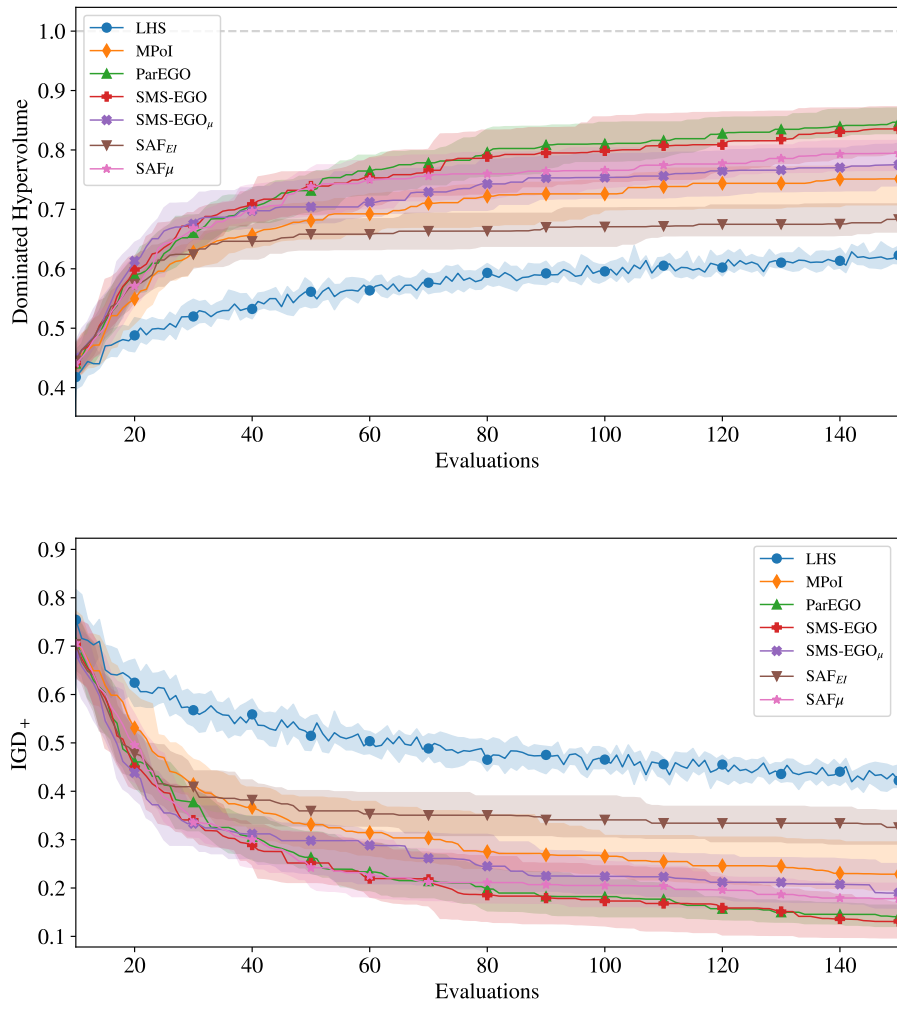
Fig. 26: Convergence plots showing median Dominated Hypervolume and IGD+ over 31 repeats. IQR shown in shaded region. Dominated hypervolume calculated as a fraction of the maximum possible.
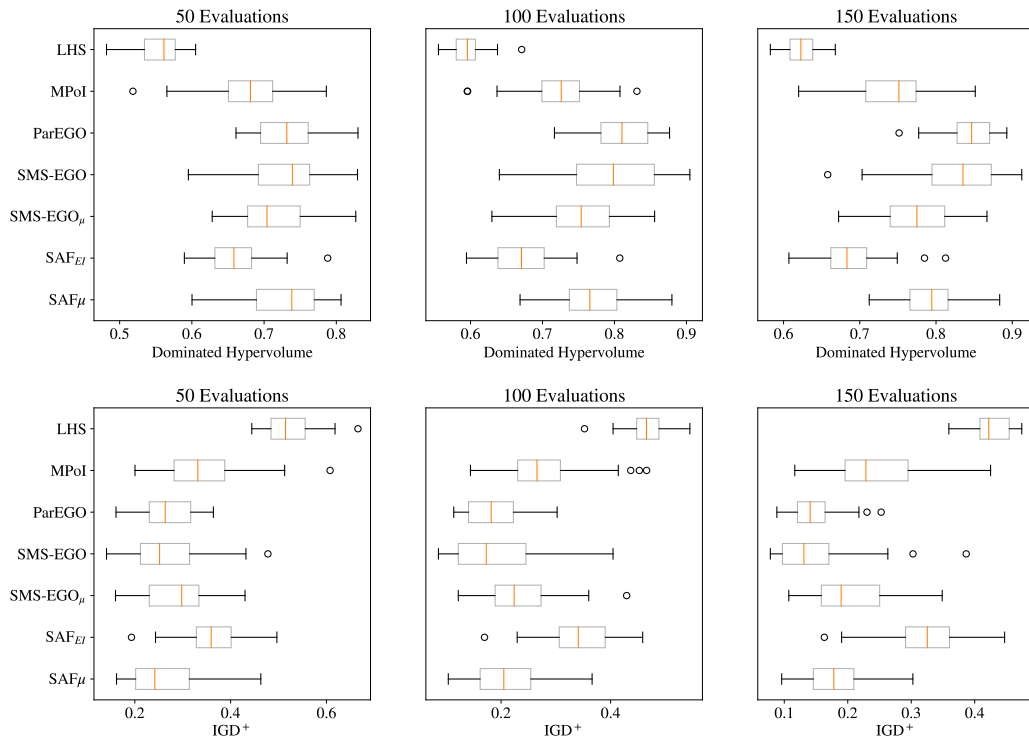

Fig. 27: Box plots showing Dominated Hypervolume and IGD+ over 31 repeats at three stages of the optimisation process.
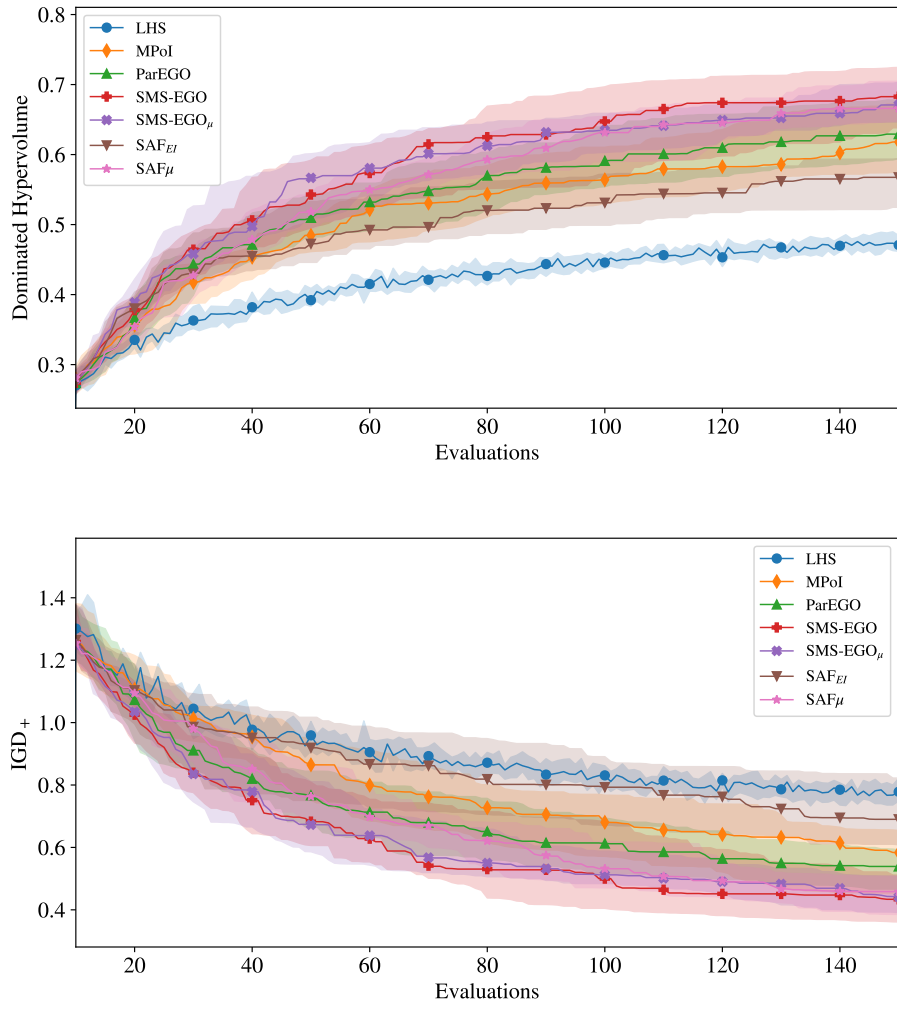
Fig. 28: Convergence plots showing median Dominated Hypervolume and IGD+ over 31 repeats. IQR shown in shaded region. Dominated hypervolume calculated as a fraction of the maximum possible.
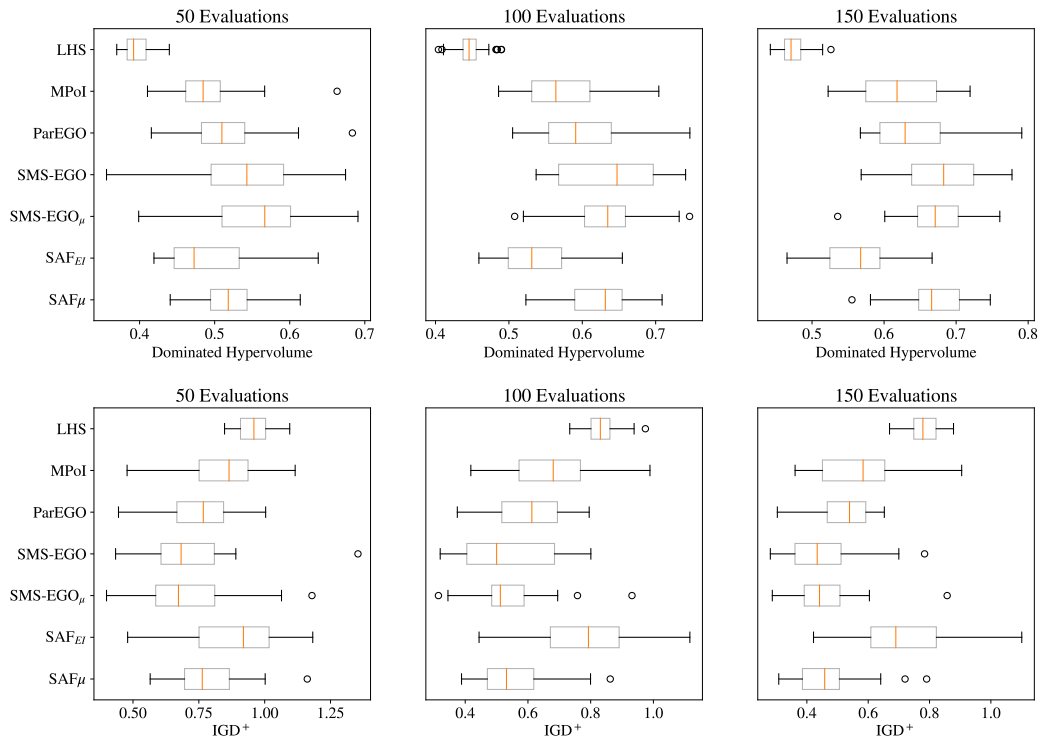

Fig. 29: Box plots showing Dominated Hypervolume and IGD+ over 31 repeats at three stages of the optimisation process.
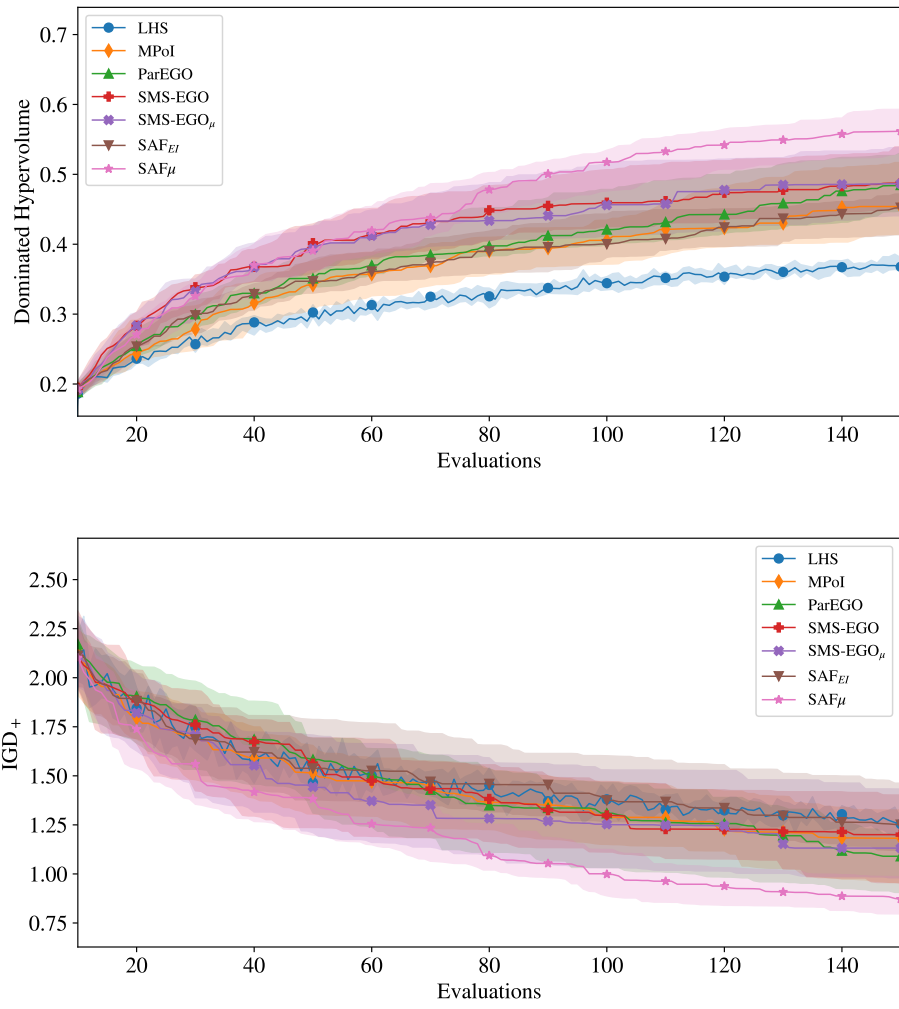
Fig. 30: Convergence plots showing median Dominated Hypervolume and IGD+ over 31 repeats. IQR shown in shaded region. Dominated hypervolume calculated as a fraction of the maximum possible.
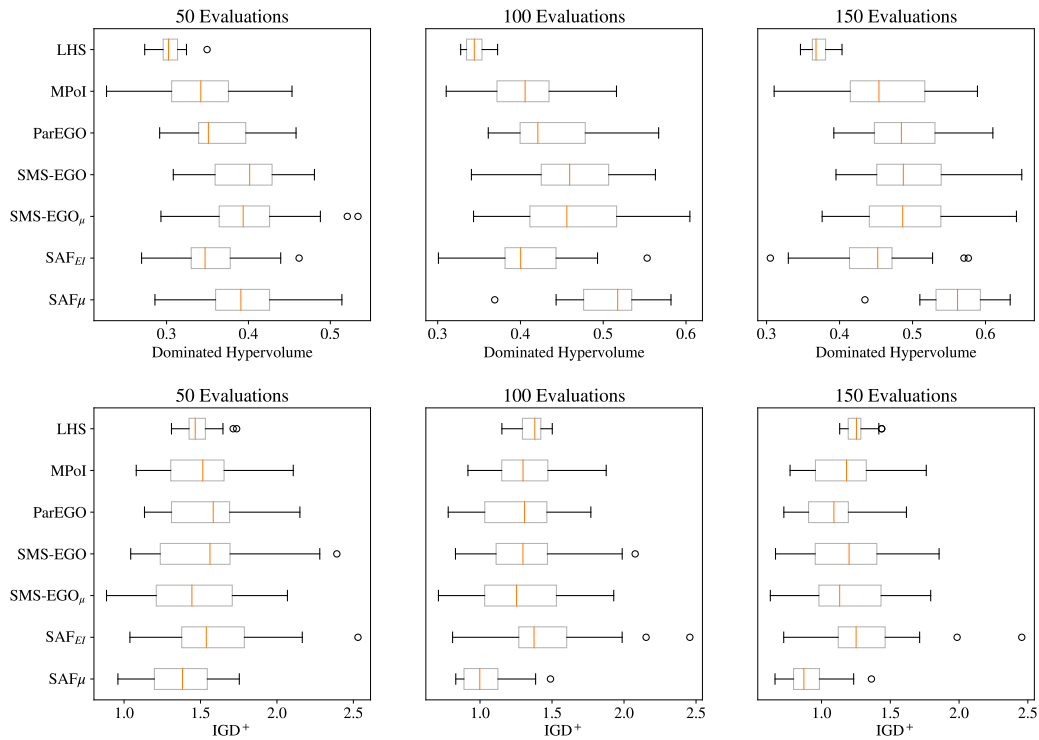

Fig. 31: Box plots showing Dominated Hypervolume and IGD+ over 31 repeats at three stages of the optimisation process.
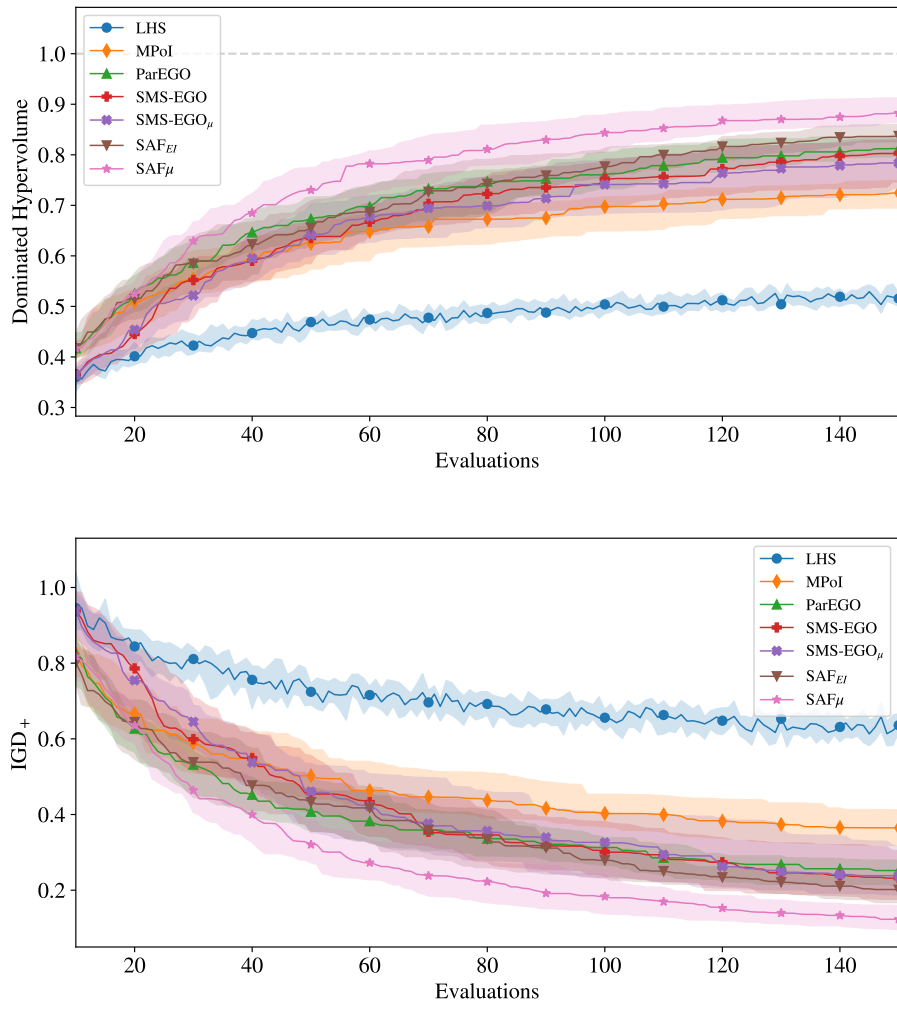
Fig. 32: Convergence plots showing median Dominated Hypervolume and IGD+ over 31 repeats. IQR shown in shaded region. Dominated hypervolume calculated as a fraction of the maximum possible.
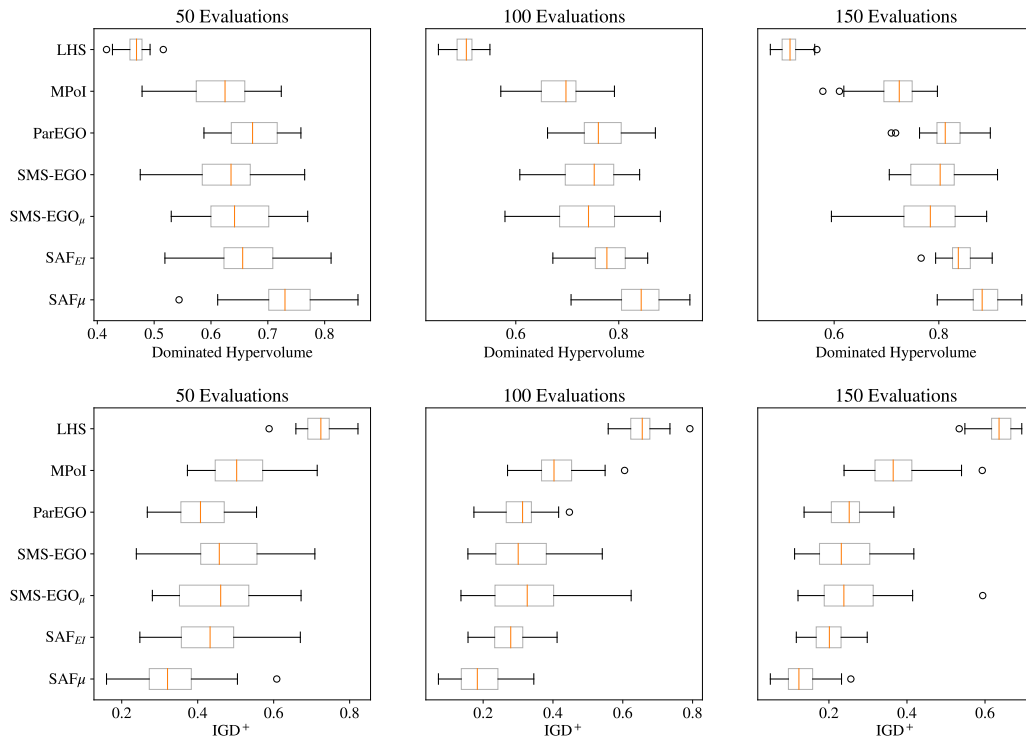

Fig. 33: Box plots showing Dominated Hypervolume and IGD+ over 31 repeats at three stages of the optimisation process.
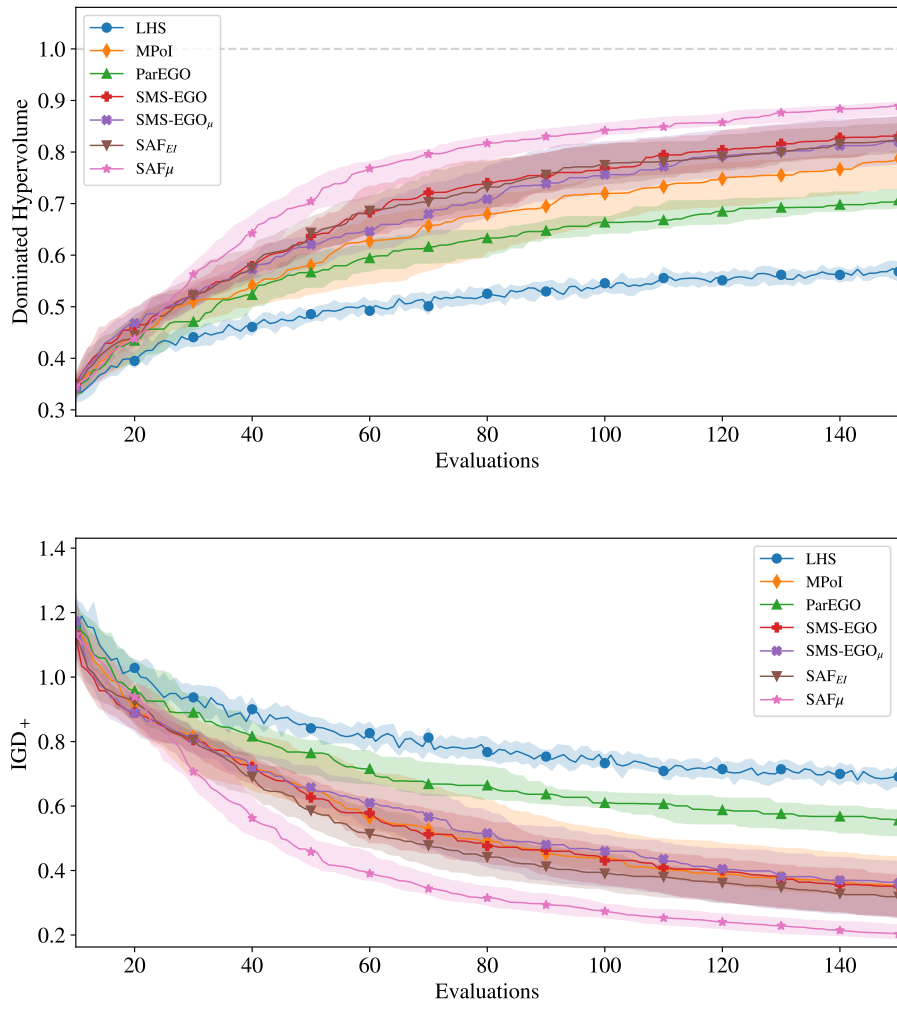
Fig. 34: Convergence plots showing median Dominated Hypervolume and IGD+ over 31 repeats. IQR shown in shaded region. Dominated hypervolume calculated as a fraction of the maximum possible.
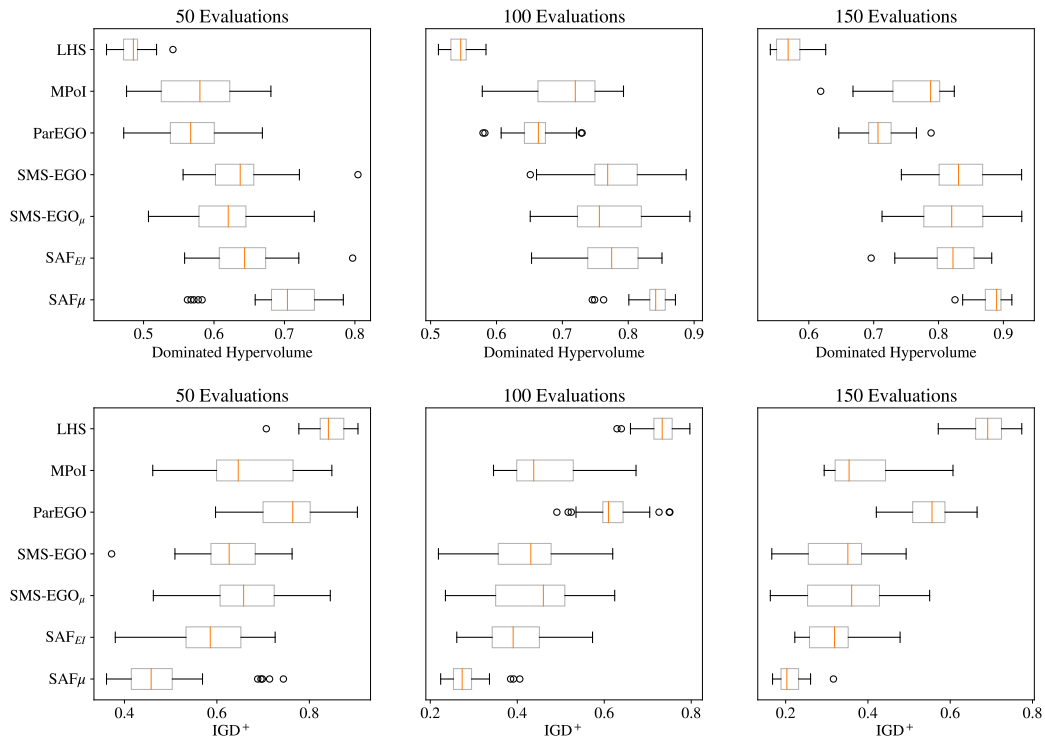

Fig. 35: Box plots showing Dominated Hypervolume and IGD+ over 31 repeats at three stages of the optimisation process.
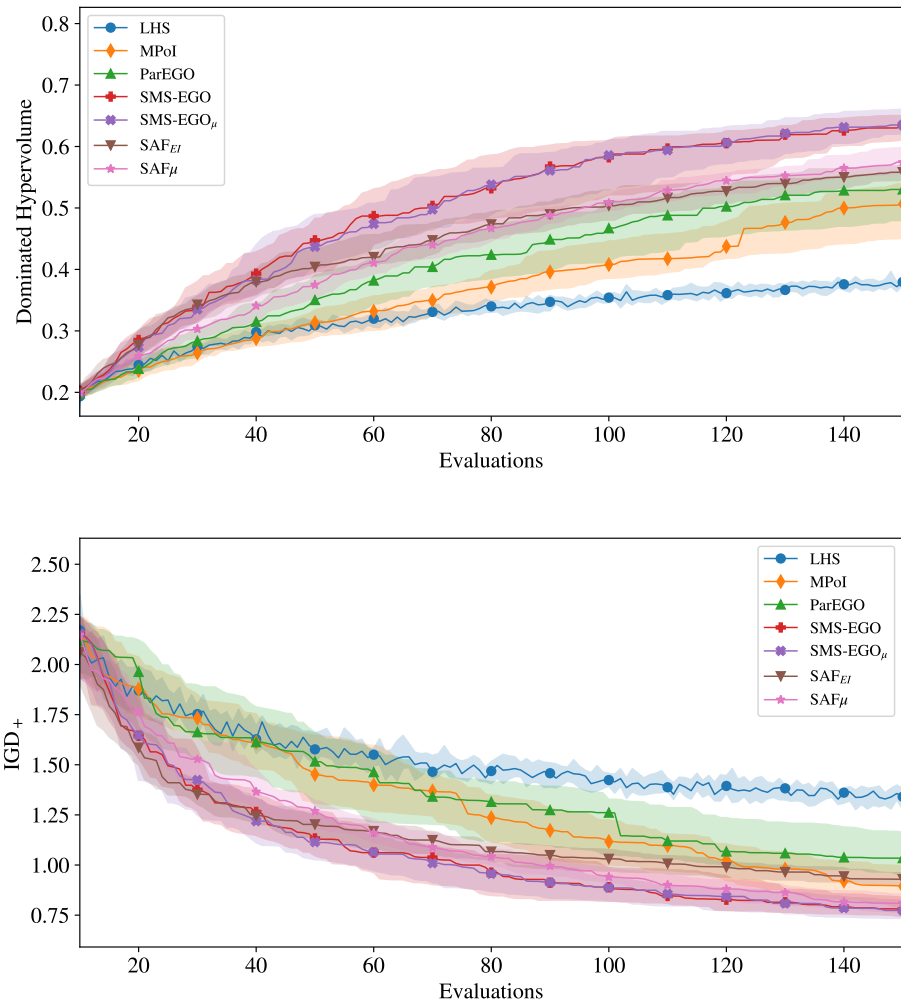
Fig. 36: Convergence plots showing median Dominated Hypervolume and IGD+ over 31 repeats. IQR shown in shaded region. Dominated hypervolume calculated as a fraction of the maximum possible.
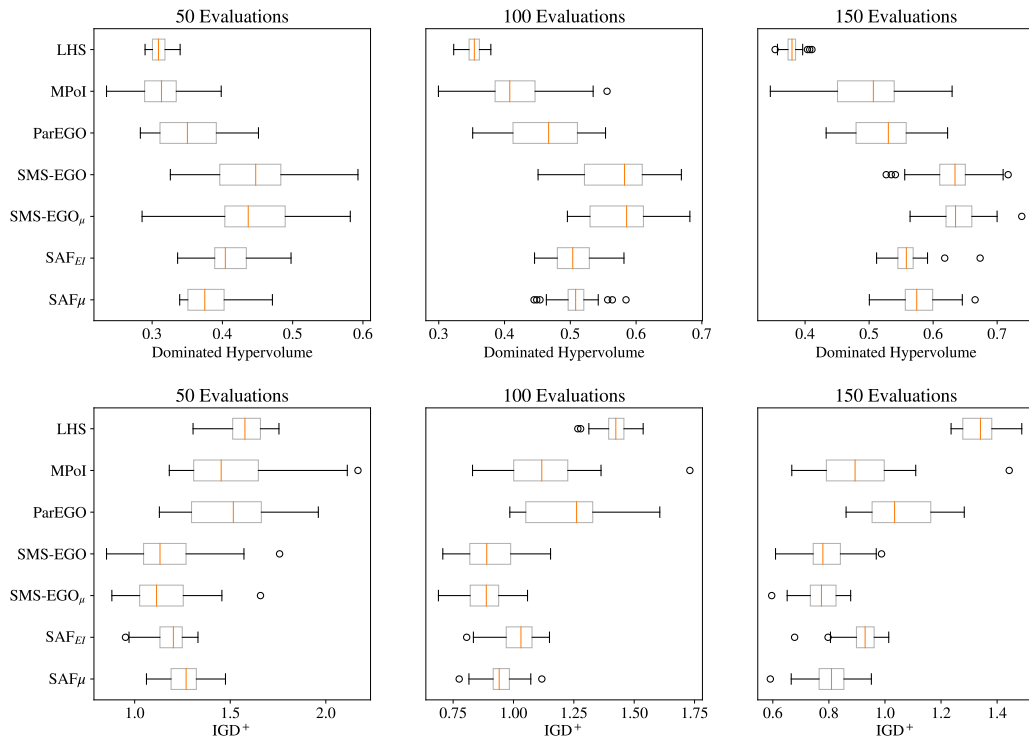

Fig. 37: Box plots showing Dominated Hypervolume and IGD+ over 31 repeats at three stages of the optimisation process.